A Detailed Theoretical Mechanism for Photographic Sensitization of the AgBr(111) Surface

Abds-Sami Malik, Francis J. DiSalvo, and Roald Hoffmann

Department of Chemistry, Cornell University, Ithaca, New York 14850

John T. Blair

Imation Corp., Oakdale Minnesota, 55128

Recent experimental characterization of the reconstructed AgBr(111) surface (a half-layer covering of Ag ions segregated into rows 7.07 Å apart) has been used to construct a theoretical model (within the framework of an approximate molecular orbital method) of that surface. Our calculations indicate that these surface Ag rows give rise to states at the bottom of the conduction band, which could serve as shallow trapping sites for photoelectrons. The theoretical model provides a mechanism for the formation of a latent image cluster through trapping of photoelectrons in the low lying state and subsequent pairwise distortion of the surface Ag within the rows to form Ag–Ag bonds. The calculations also indicate that substantial electron transfer from the ionic extreme occurs in both the bulk and surface models.

Journal of Imaging Science and Technology 42: 210–215 (1998)

Introduction

Silver halides have been the basis for photography for over 150 years. Since the first faint images produced by Niepce in the 1830s, incredible improvements have been made to photographic technology. Still, one wishes we understood the physical and chemical mechanisms of the process better—a sound theoretical framework describing photography in microscopic detail has been taking shape much slower than the empirical advances in film quality and sensitivity. In a modest contribution to the field, the present work uses an approximate olecular orbital method, the extended Hückel theory, to explore the mechanism of latent image formation on the AgBr(111) surface. In our analysis, we will invoke some of the ideas of photoelectrons and trapping sites first expounded by Gurney and Mott.[1] The method we employ is able to describe the electronic structure of a AgBr(111) surface in some detail and shows the evolution of electronic levels as a latent image cluster is formed.

Calculations were done on bulk AgBr and on the AgBr(111) reconstructed surface. The approximate molecular orbital method used and its parameters are described in the Appendix, as are details of the geometry used. The bulk and surfaces are calculated by three- and two-dimensional band structure calculations using the extended Hückel method. This is an approximate molecular orbital method with well-recognized limitations. While the method does not predict absolute energies well, it does capture the general bonding characteristics of a wide range of discrete and extended structures. Theoretical densities of states (DOS)[2b] and crystal orbital overlap population (COOP)[2c] curves will figure importantly in our analysis. Throughout this article we use Ag and Br as symbols for atom types, without any implication as to the specific ionicity of these centers.

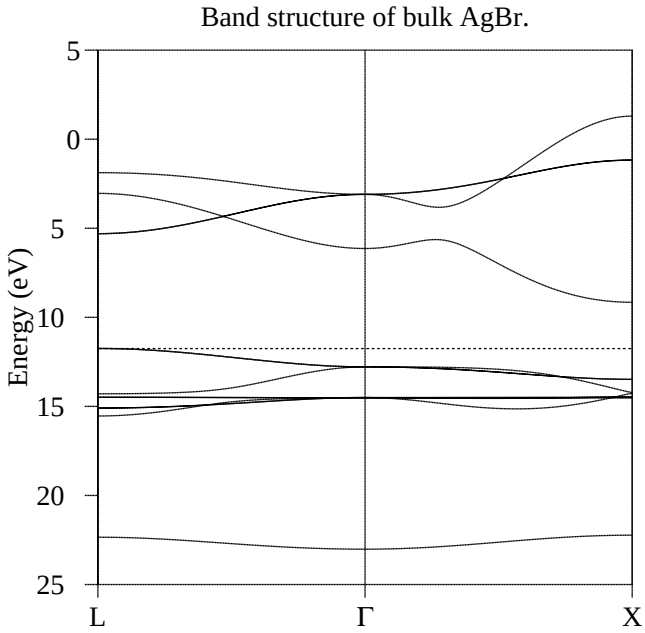

Figure 1. The band structure of bulk AgBr from Γ to *X* and from Γ to *L*.

Original manuscript received May 29, 1997

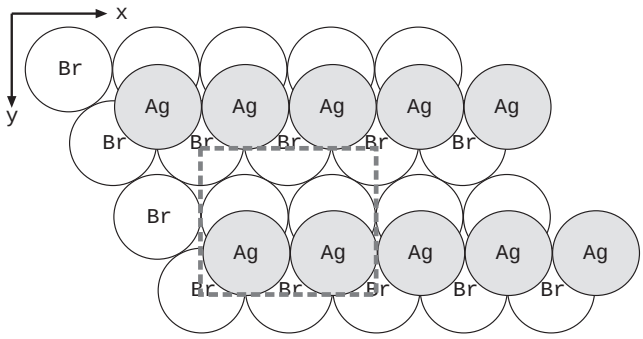

Figure 2. The AgBr(111) reconstructed surface. The surface silver half-layer segregates into rows that are 7.07 Å apart. The Ag–Ag distance within the rows is 4.08 Å. The unit cell that was used in the calculations is outlined by a dashed line.

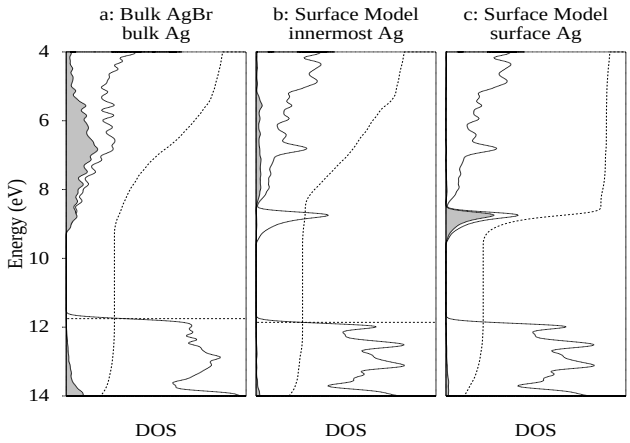

Figure 3. The horizontal dashed line is the Fermi level. The solid line is the total DOS: the shaded region is the contribution to the total DOS of the specified Ag *s*–orbital. The dotted curve is the integral of the specified DOS contribution: (a) bulk AgBr, bulk Ag; (b) surface model, innermost Ag; (c) surface model, surface Ag.

Bulk Silver Bromide and the Silver Bromide Surface

Figure 1 shows the calculated band structure for bulk AgBr. The calculation was done using a primitive unit cell. The bands are shown in the directions Γ to *X* and Γ to *L* (*X* = 0.5, 0, 0; *L* = 0.5, 0.5, 0.5) in the Brillouin zone. Our method reproduces reasonably the results of earlier calculations[3–5] and is in approximate agreement with experimental data,[6] for instance, in the calculated band gap of 2.5 eV. There is a surprise, however; in our calculations, the Ag and Br emerge carrying average net charges of ±0.034, respectively, far from the ionic extreme of ±1.

Current methods of assigning electron density to atoms in a calculation carry some degree of arbitrariness. We use the Mulliken "population analysis," one much applied, uniquely defined, but arbitrary way of dividing electron density between atoms.[2a] Other population analyses (equally arbitrary) will give different ionicities. It is, nevertheless, clear that in AgBr there are a good many occupied Ag *s* and *p* states. This leads to a nonionic model for silver bromide. We think that this is likely to be true in other calculations. We realize that the finding of a significant degree of covalency in bulk silver bromide will not be accepted easily by many in the photographic community.

AgBr crystallizes in the rock salt structure type; therefore an ideal (111) surface consists entirely of Br or Ag. It had been postulated for some time[7] that this ideal surface undergoes a reconstruction to give a half-layer covering of Ag or Br. Several models, based on theoretical calculations as well as experimental data, have been proposed for this reconstruction.[8–11] These models agree that the surface should be a half–layer covering of ions. But considerable disagreement exists over which species (Ag or Br) is on the surface and over the exact nature of the reconstruction. However, some recent studies of the AgBr(111) surface, using SEXAFS spectroscopy have shown that the reconstruction is a row type segregation of Ag on the surface.[12,13] In this model, shown in Fig. 2, one sees chains of Ag ions, 4.08 Å apart within a chain and separated by 7.07 Å between the chains.

The AgBr(111) surface was modeled using a seven interior layer slab with the reconstructed Ag ions placed on both surfaces, in positions suggested by experimental work.* An interesting feature of the surface model is that the net charges on Ag and Br vary in relation to their distance from the surface. At the middle of the slab, the charges are ±0.035; similar to those calculated earlier for bulk AgBr. However, at the surface, the ionicity of the Ag is quite different. The charge on the reconstructed Ag at the surface is +0.35; ten times that of Ag in the bulk. The Ag centers one layer below carry a charge of +0.05. This finding suggests that the ionicity of Ag in microcrystals of AgBr will vary with respect to their distance from the surface. The Ag at or near the surface will be more ionic in character than Ag in the bulk.

Figure 3 shows the calculated DOS for both three-dimensional bulk AgBr and the reconstructed two-dimensional AgBr(111) surface model. The shaded region of each DOS plot indicates the contribution (or projection) of Ag *s*–states to the total DOS. There is also a dotted integration line, which indicates the total fraction of the projected states up to a given energy. The Ag *s*–states are very much dispersed throughout the conduction band, and also appear, to a smaller extent in the valence band (which is mainly Br).

The surface model calculations [Fig. 3(b) and 3(c)] show something new, a peak in the DOS near –9.10 eV, the bottom of the conduction band. Such a peak is not present in the case of bulk AgBr [Fig. 3(a)]. Intrigued by this new feature, we investigated its origins. Two types of Ag are present in the slab, interior (three such layers) and surface (two half–layers); the contribution of the Ag *s*–states from the one innermost layer (i.e., most bulk-like layer) and from the surface layer to the total DOS is shown in Fig. 3(b) and Fig. 3(c), respectively. The interior Ag *s*–states are quite dispersed throughout the valence and conduction bands, analogous to bulk AgBr. However, the surface Ag *s*–states are very much localized to that new peak at the bottom of the conduction band. The narrowness of this peak is an indication of the localization of these states in real space.[2d] The location of this peak in the vicinity of the band gap is ideal for it to serve as a shallow trap for a photoelectron.

The Latent Image

At this point we summarize briefly current ideas about the photographic process and some of its terminology. Some of the relevant basic concepts were first introduced by Gurney and Mott,[1] and modified later by Mitchell, Hamilton, and others.[14c] A latent image forms after exposure of film to light. This latent image is then amplified during the development process to produce the final photographic

* A seven layer slab was found to be sufficient to model bulk-like properties in the innermost layers. This was probed by comparing the DOS and atomic charges of the innermost layers with the values obtained from a calculation on bulk AgBr. Please see the Appendix.

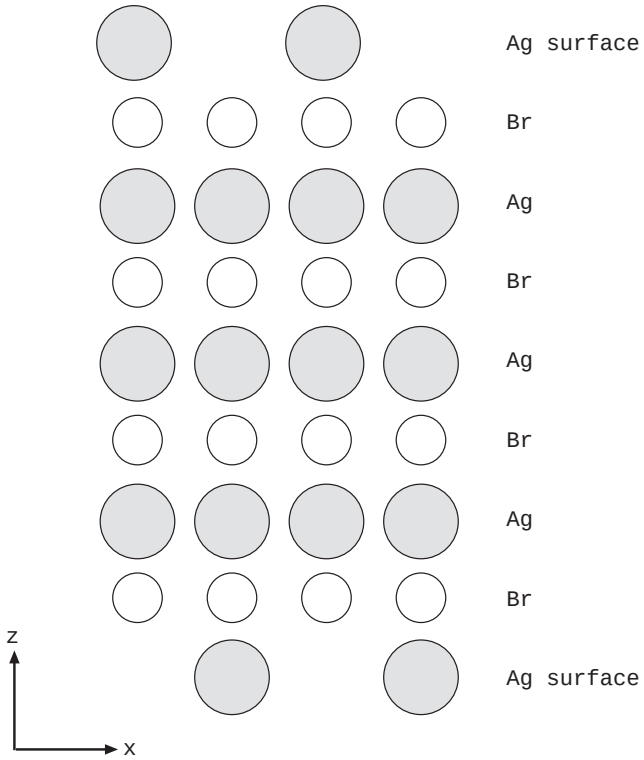

Figure 4. A schematic drawing of the seven layer slab model used in the calculations.

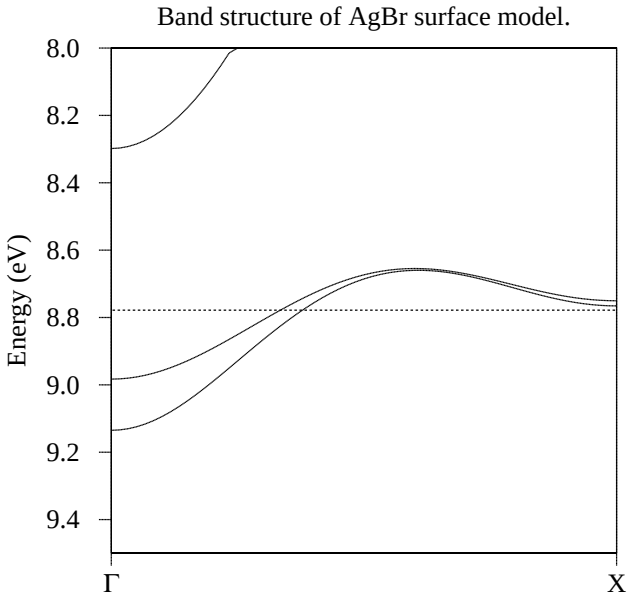

Figure 5. The surface Ag *s*–band as calculated from Γ to *X* for the geometry of Fig. 2. The Fermi level is indicated for the case of one photoelectron trapped per surface Ag. In this energy window only the bands arising from primarily surface Ag atoms are visible.

image. It is thought that the latent image consists of clusters of Ag atoms on the AgBr surface. These are termed "latent image clusters" and typically consist of 4 to 5 metal atoms.[14a,15]

Current mechanisms of latent image formation propose that exposure of AgBr to light produces a photoelectron and a hole. The photoelectron then becomes trapped at a trapping site. An interstitial Ag^+ ion is attracted to this site and reduced to neutral Ag, forming a latent pre–image center. This neutral Ag, it is thought, is able to capture another photoelectron and then attract another interstitial Ag^+ ion from the bulk to form Ag_2. The Ag_2 is called a "latent subimage center" and is stable whereas the latent pre–image center is not stable.[14c] The process is then repeated several times to form a large latent image cluster. This is known as the "nucleation and growth" model.

The formation of a latent subimage center is necessary to the growth of a latent image cluster. Unspecified in this model is the nature of the trapping site, the detailed structure and stability of the latent subimage center, and the mechanism for Ag-Ag bond formation during the creation of the subimage center. These points are our main concern here.

Distortion of the Surface Silver Ion Chains

Returning to our computational model, consider the possibility of photoelectrons trapped in the surface Ag *s*–state we have found in our calculations. Figure 5 shows the band structure from Γ to *X* (not the entire Brillouin zone) for the surface model in the energy window from –8.0 to –10.0 eV. Before we had shown only the resulting DOS. The two complete bands shown are the ones responsible for the peak in the DOS of interest to us; they are largely made up of surface Ag *s*–orbitals.† The Fermi level indicated is now for the case of one photoelectron trapped per one surface Ag. In other words, we have included enough electrons to half populate the surface Ag *s*–state, and formally reduce all of the surface Ag ions to neutral Ag atoms.‡

It is apparent that along this direction in the Brillouin zone one has a half–filled band (or two bands). Such a situation points to a potential Peierls distortion,[2e] a motion of the atoms of the lattice that opens up a band gap at the point of filling. There are many ways of realizing a Peierls distortion, and unfortunately the extended Hückel method is not reliable for optimizing distances. We reasoned that a pairing distortion should keep as many surface Ag–Br separations constant as possible, and so came upon the motion illustrated in Figs. 6 and 7. Pairs of surface Ag are moved diagonally toward each other while keeping all the Br positions unchanged. In the undistorted model, the three closest Br to surface Ag distances are all 2.89 Å. The distortion studied keeps two of these Ag–Br distances constant while the third Ag–Br distance (the Br that the Ag is moving away from) increases. This is not the only deformation possible, but we believe that it is a plausible one.

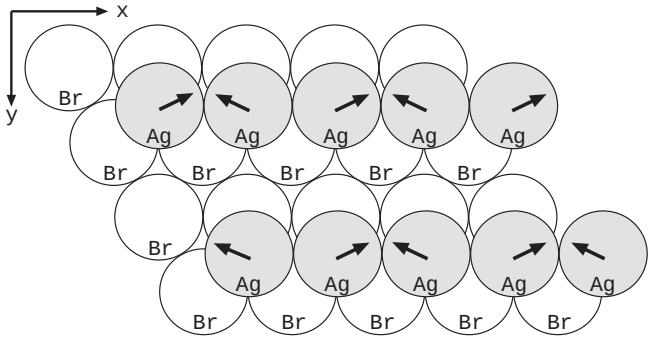

Figure 6. The proposed distortion of the surface Ag is indicated by the arrows.

† Two s-bands arise because in our model we have two surfaces. The fact that the bands are not completely degenerate throughout the Brillouin zone is due to the weak coupling of the surface states through the seven intervening layers.

‡ This is the most extreme case. The calculations with fewer photoelectrons are discussed later.

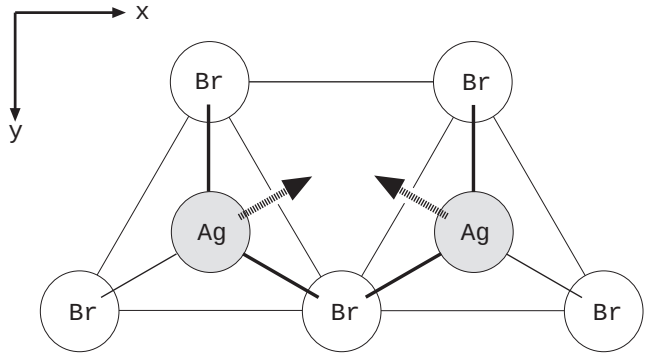

Figure 7. A more detailed illustration of the proposed distortion of the surface Ag. The motion of surface Ag is indicated by the dashed arrows. The Ag–Br distances that are kept constant are drawn with heavy lines.

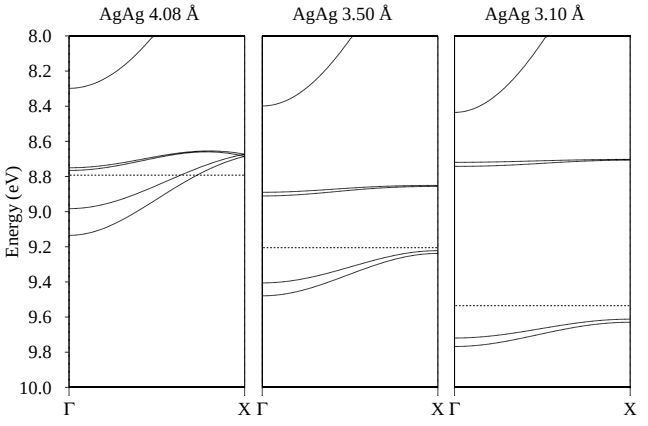

Figure 8. The surface Ag *s*–band is calculated from Γ to *X* as the Peierls distortion indicated in Fig. 6 occurs. The leftmost panel shows the band structure for the undistorted surface. The band structure for the closest surface Ag–Ag distance is shown in the rightmost panel. The Fermi level in all cases has been calculated from the studied two-dimensional model discussed in the text.

To model this distortion in the calculations, the unit cell was doubled in the x–direction. This leads to the phenomenon of bands "folding back".[2e] The leftmost band structure in Fig. 8 is actually that of the undistorted surface prepared for subsequent deformation; the levels this band structure contains (in a halved Brillouin zone) are exactly the same as in Fig. 5. Calculations were done on a doubled unit cell for surface Ag–Ag distances ranging from 4.08 Å (undistorted) to 3.10 Å with one photoelectron trapped per Ag ion on the surface (i.e., reducing all the surface silver ions to formally neutral silver). As Fig. 8 shows the lower bands are stabilized in energy while the upper, empty bands are destabilized. The Fermi level indicates that the lower pair of bands is filled.

One should not conclude from the clear splitting of the surface Ag *s*–bands indicated in Fig. 8(a) through 8(c) that the system becomes an insulator. The band splitting occurs where it should, along the Γ to *X* direction maximally affected by the pairing distortion. Along other directions in the zone (Γ–Y–M–Γ, not shown here) less change occurs in the level energies with distortion, and a good number of states remain near the Fermi level. The evolution of the total DOS (Fig. 9) shows this, but also indicates clearly a stabilization with pairing, for the reasons we have analyzed.

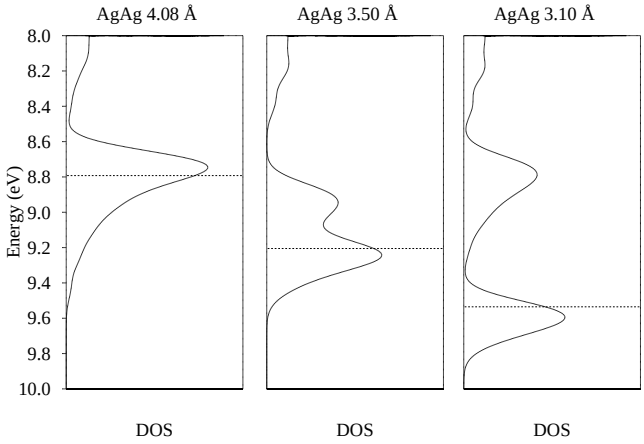

Figure 9. This DOS corresponds to the band structure shown in Fig. 8.

Energetics and Bond Formation for Reduced Silver Bromide Surfaces

To gauge the stabilization upon Ag–Ag surface pairing and the corresponding growth in strength of some surface Ag–Ag bonds, calculations were done as described previously, varying the surface Ag–Ag distances from 4.08 to 3.10 Å, for the following cases: no electrons per two surface silvers, one extra electron per two surface silvers, and two extra electrons per two surface silvers. The latter two cases are essentially modifications of electron counts (or number of photoelectrons).

Our concern is with the extent of Ag–Ag bonding, so it is important to have a model for such bonding. Two neutral Ag atoms should give us a model of a Ag–Ag single bond, and two Ag^+ ions should interact only weakly. As a calibration, the following calculations were done for diatomic *molecules*, specifically: two Ag^+ ions interacting, one Ag^0 and one Ag^+ interacting, and two Ag^0 interacting. The overlap population (OP) and net energy stabilization for each case was calculated. These results are summarized in Figs. 10 and 11.

The reference system of Ag^+–Ag^+, which one might expect to be repulsive (d^{10}–d^{10}), is actually slightly attractive (in energy) and bonding (judged by the OP). The reason for this phenomenon has been discussed for Cu^+–Cu^+, we have suggested that it is due to *s*, *p* orbital mixing into the *d* block.[16,17] Other explanations for such d^{10}–d^{10} attractions in coinage metals have been proposed.[18]

For these model diatomics, the overlap population and relative energy stabilization indeed increase as one goes from Ag^+–Ag^+ to Ag^0–Ag^+, and are greatest for two Ag^0 interacting. Turning to the surface calculations, as far as the OPs are concerned, this trend is reflected for two surface silvers pairing. Figure 10 shows that the overlap population is greater for two electrons per two surface Ag than for one electron per two Ag and is lowest for no electrons per two Ag.

The general trend is followed for the relative stabilization energy, as shown in Fig. 11. Greater energy stabilization exists for the case of two electrons per two Ag than for one electron per two Ag, though the deformation seems initially to encounter a small barrier. The other case also follows the general trend observed in the overlap populations.

Concluding Remarks

Our purpose has to suggest a mechanism for the formation of a subimage cluster. Previous researchers postulated

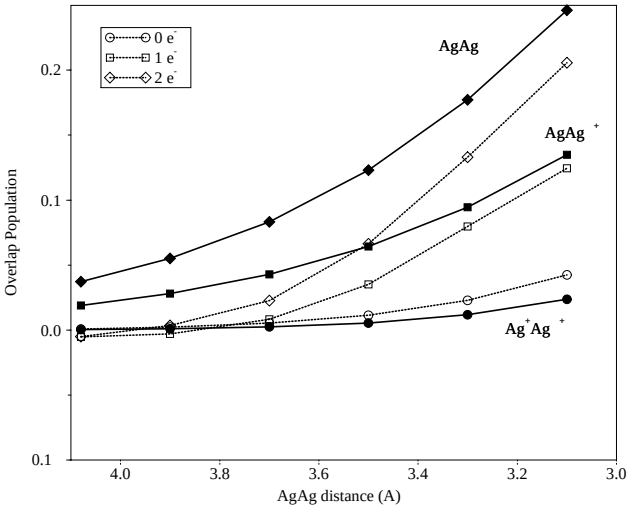

Figure 10. Overlap population plots. The solid curves correspond to diatomic molecular models: two Ag, two Ag^+, or one Ag and one Ag^+ atoms interacting. Each line is appropriately labeled directly on the graph. The dotted curves correspond to two Ag atoms on the AgBr surface interacting, with various choices for the number of additional electrons per pair of surface Ag atoms. Each case discussed in the text is labeled in the legend.

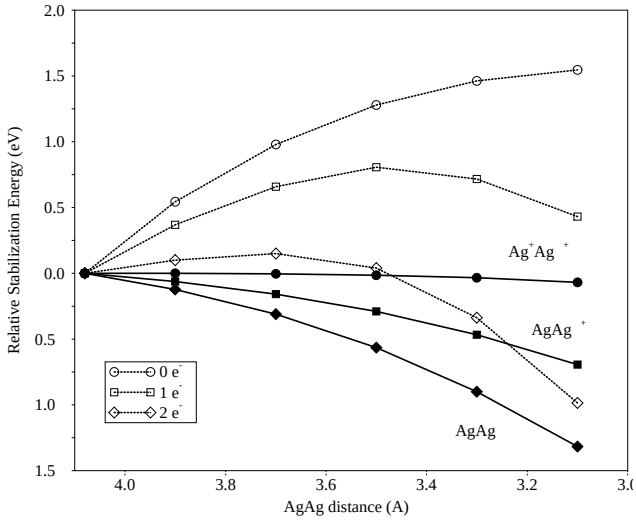

Figure 11. Relative energy stabilization plots. The solid curves correspond to two Ag, two Ag^+, or one Ag and one Ag^+ interacting. Each line is appropriately labeled directly on the graph. The dotted curves correspond to two Ag on the AgBr surface interacting. Each case discussed in the text is labeled in the legend.

the existence of "shallow trapping sites"[19] for photoelectrons on the surface of AgBr. It was believed also that after the trapping of a photoelectron an Ag^+ ion would migrate to this site followed by capture of another photoelectron and the migration of another Ag^+ to form the Ag_2 latent subimage center. However, the exact nature of the trapping site and mechanism for formation of a subimage cluster was not specified. Our model has identified the trapping site as a band of levels, a reconstructed surface Ag *s*–state, which lies just below the bulk conduction band.

We have further provided an alternative mechanism and a rationale (through Peierls distortion) for the formation of a subimage cluster. This model suggests that stabilized, reduced Ag–Ag pairs form on the surface.

This band of levels is ideal for interaction with dye molecules. Theoretical investigations of dye molecules interacting with these surface states would provide valuable insights into how the electronic levels of AgBr are modified by dye molecules.

With our method of dividing electrons among atoms, bulk AgBr came out hardly ionic. But the degree of ionicity near the AgBr(111) surface was found to be greater than in the bulk. This is consistent with experimental observations that the ionic conductivity of AgBr microcrystals and AgBr(111) thin films are greater than that of bulk AgBr.[14a,20,21] There are more cationic charge carriers near the surface. These results suggest that in future investigations, the differences in ionicity between bulk and surface AgBr should be taken into account. Investigations into the AgBr(100) surface states are currently underway; studies of Au and S influence on photographic sensitivity will be published separately.

Acknowledgements. We are grateful to Imation for its support of our work through a grant to Cornell University. William A. Bernett of 3M was instrumental in getting this collaboration started and we thank him.

TABLE I. Extended Hückel Parameters Used

Atom	Orbital	H_{ii} (eV)	ζ_1	ζ_2	C_1	C_2
Ag	5s	–10.5	2.244			
	5p	–5.8	2.202			
	4d	–14.5	6.07	2.663	0.5591	0.6048
Br	4s	–22.07	2.588			
	4p	–13.1	2.131			

Appendix

All calculations were done using the extended Hückel method, a semi-empirical molecular orbital method[22] with the program YAeHMOP by Greg Landrum. The parameters are given in Table I. The unit cell used in the two-dimensional calculations is outlined in Fig. 2 by a dashed line. The unit cell for the two-dimensional calculations consisted of 32 or 34 atoms (depending on whether Au was included or not).

DOS and band structure calculations of bulk (3-D) AgBr were done with a primitive unit cell and were compared with previous calculations[3–5] done using other techniques. The extended Hückel calculations on bulk AgBr reproduced the earlier results.

The seven layer slab model for the surface was chosen after doing calculations on a series of models having from 5 to 12 layers. In each model, the DOS and the average net charges on the atoms in the innermost layers were compared with values obtained from the calculation on bulk AgBr. It was found that seven layers were sufficient to model bulk properties in the innermost layer.

References

1. R. Gurney and N. Mott, *Proc. R. Soc. Lond. Ser. A* **164**, 151 (1938).
2. R. Hoffmann, Solids and Surfaces: A Chemist's View of Bonding in Extended Structures, VCH Publishers, New York, 1988, (a) pp. 32–36; (b) 36–42; (c) 42–45; (d) 62–63; (e) 92–95.
3. A. B. Kunz, *Phys. Rev. B* **26**, 2070 (1982).

4. A. Gordienko, Y. N. Zhuravlev, and A. Poplavnoi, *Phys. Stat. Sol b* **168**, 149 (1991).
5. B. Onwuagba, *Sol. State Commun.* **97**, 267 (1996).
6. F. C. Brown, *J. Phys. Chem.* **66**, 2368 (1962).
7. J. Hamilton and L. Brady, *Surf. Sci.* **23**, 389 (1970).
8. R. C. Baetzold, Y. T. Tan, and P. W. Tasker, *Surf. Sci.* **195**, 579 (1988).
9. H. Haefke and M. Krohn, *Surf. Sci. Lett.* **261**, L39 (1992).
10. G. Hegenbart and T. Müssig, *Surf. Sci. Lett.* **275**, L655 (1992).
11. H. Hofmeister, S. Grosse, G. Gerth, and H. Haefke, *Phys. Rev. B* **49**, 7646 (1994).
12. P. Tangyunyong, T. Rhodin, Y. Tan, and K. Lushington, *Surf. Sci.* **255**, 259 (1991).
13. Y. Tan, K. Lushington, P. Tanyunyong, and T. Rhodin, *J. Imaging Sci. Technol.* **36**, 118 (1992).
14. T. Tani, *Photographic Sensitivity: Theorty and Mechanisms* (Oxford University Press, New York, 1995), (a) pp. 48–59; (b) 81–87; (c) 91–95.
15. R. Hailstone and J. Hamilton, *J. Imaging Sci.* **29**, 125 (1987).
16. P. K. Mehrotra and R. Hoffmann, *Inorg. Chem.* **17**, 2187 (1977).
17. K. M. Merz, Jr., and R. Hoffmann, *Inorg. Chem.* **27**, 2120 (1988).
18. P. Pyykkö, *Chem. Rev.* **97,** 597 (1997).
19. A. P. Marchetti and R. S. Eachus, In *Advances in Photochemistry*, D. H. Volman, G. S. Hammond, and D. C. Neckers, Eds., John Wiley and Sons, New York, 1992, pp. 145-216.
20. R. C. Baetzold and J. F. Hamilton, *Surf. Sci.* **33**, 461 (1972).
21. R. C. Baetzold and J. F. Hamilton, *Surf. Sci.* **179**, L85 (1987).
22. R. Hoffmann, *J. Chem. Phys.* **39**, 1397 (1963).